Journal of Experimental Botany, Vol. 61, No. 1, pp. 131–142, 2010
doi:10.1093/jxb/erp301 Advance Access publication 3 November, 2009
This paper is available online free of all access charges (see http://jxb.oxfordjournals.org/open_access.html for further details)

Journal of Experimental Botany
www.jxb.oxfordjournals.org

RESEARCH PAPER

The constitutive expression of *Arabidopsis* plasmodesmal-associated class 1 reversibly glycosylated polypeptide impairs plant development and virus spread

Raul Zavaliev[1], Guy Sagi[1], Abed Gera[2] and Bernard L. Epel[1,*]

[1] Department of Plant Sciences, George S Wise Faculty of Life Sciences, Tel Aviv University, Tel Aviv 69978, Israel
[2] Department of Plant Pathology, Agricultural Research Organization, The Volcani Center, Bet Dagan 50250, Israel

Received 23 July 2009; Accepted 3 September 2009

Abstract

***Arabidopsis* class 1 reversibly glycosylated polypeptides (^{C1}RGPs) were shown to be plasmodesmal-associated proteins. Transgenic tobacco (*Nicotiana tabacum*) plants constitutively expressing GFP tagged AtRGP2 under the control of the CaMV 35S promoter are stunted, have a rosette-like growth pattern, and in source leaves exhibit strong chlorosis, increased photoassimilate retention and starch accumulation that results in elevated leaf specific fresh and dry weights. Basal callose levels around plasmodesmata (Pd) of leaf epidermal cells in transgenic plants are higher than in WT. Such a phenotype is characteristic of virus-infected plants and some transgenic plants expressing Pd-associated viral movement proteins (MP). The local spread of *Tobacco mosaic virus* (TMV) is inhibited in *AtRGP2:GFP* transgenics compared to WT. Taken together these observations suggest that overexpression of the AtRGP2:GFP leads to a reduction in Pd permeability to photoassimilate, thus lowering the normal rate of translocation from source leaves to sink organs. Such a reduction may also inhibit the local cell-to-cell spread of viruses in transgenic plants. The observed reduction in Pd permeability could be due to a partial Pd occlusion caused either by the accumulation of AtRGP2:GFP fusion in Pd, and/or by constriction of Pd by the excessive callose accumulation.**

Key words: Callose, plasmodesmata, reversibly glycosylated polypeptide, starch accumulation, stunting, *Tobacco mosaic virus*, virus spread.

Introduction

Direct cell-to-cell communication in plants is through plasmodesmata (Pd), coaxial membranous channels that span cell walls interconnecting the cytoplasm, plasma membrane (PM), and endoplasmic reticulum of contiguous cells. Pd function in the intercellular transport of a wide range of solutes, proteins, RNA, and signalling molecules and are exploited by viruses as a conduit for viral spread (Heinlein and Epel, 2004). The cell wall surrounding Pd is modified, being devoid of cellulose and hemicellulose and is composed, in part, of non-esterified pectin, callose, other non-cellulosic polyglucans, and probably, as yet uncharacterized, proteins.

During the last few years there have been various studies aimed at characterizing Pd composition (Epel *et al.*, 1995; Bayer *et al.*, 2004; Faulkner *et al.*, 2005; Lee *et al.*, 2005; Sagi *et al.*, 2005; Levy *et al.*, 2007; Thomas *et al.*, 2008). Proteomic analyses of isolated cell walls and of an enriched Pd fraction led to the identification of a class 1 reversibly glycosylated polypeptide (Epel *et al.*, 1996; Sagi *et al.*, 2005) and a β-1,3-glucanase (Levy *et al.*, 2007) as plasmodesmal associated proteins. Reversibly glycosylated polypeptides (RGPs) are highly conserved plant-specific proteins that can be subdivided into two classes, Class 1 and Class 2 RGPs (^{C1}RGPs and ^{C2}RGPs, respectively) (Langeveld *et al.*, 2002). ^{C1}RGPs were found to be associated with cell walls, specifically Pd (Epel *et al.*, 1996; Sagi *et al.*, 2005), and with *trans*-Golgi vesicles (Epel *et al.*, 1996; Dhugga *et al.*, 1997; Sagi *et al.*, 2005; Drakakaki *et al.*, 2006). They form large

* To whom correspondence should be addressed: E-mail: blepel@post.tau.ac.il

hetero- and homomultimeric complexes (Langeveld *et al.*, 2002; De Pino *et al.*, 2007) and are reversibly autoglycosylated with nucleotide sugars UDP-glucose, UDP-xylose, and UDP-galactose (Dhugga *et al.*, 1991, 1997; Delgado *et al.*, 1998; Langeveld *et al.*, 2002; Testasecca *et al.*, 2004). Since RGPs do not possess any signal peptide, the mechanism of their delivery to Golgi apparatus remains unknown. However, it was surmised that the ^{C1}RGPs are transported to Pd by Golgi, bound to the outer Golgi vesicle membrane as a peripheral protein and that the protein, upon association with the plasmodesmal-PM, faces the cytoplasmic sleeve (Sagi *et al.*, 2005).

^{C1}RGPs have been assumed to be involved in matrix cell wall polysaccharides biosynthesis (Dhugga, 2006). Direct evidence, however, is lacking. The *Arabidopsis* (*Arabidopsis thaliana*) genome contains four members of ^{C1}RGPs (AtRGP1–4) (Langeveld *et al.*, 2002). Heterologous expression of ^{C1}RGPs from *Arabidopsis* (AtRGP1–4) in tobacco (*Nicotiana tabacum*) showed specific association with wall regions containing Pd (or pit fields) and data were presented that suggest that they are delivered to this compartment by *trans*-Golgi vesicles (Sagi *et al.*, 2005). The role of association with Pd is yet unknown, but it seems that this association is a general feature of these proteins since a close homologue of RGP was also identified from the multicellular green alga *Chara corallina* in a proteomic analysis of nodal cell walls which contain Pd, but not from internodal cell walls which lack Pd (Faulkner *et al.*, 2005), and a GFP fusion of a ^{C1}RGP from *Solanum lycopersicum* also appears to associate with Pd (Selth *et al.*, 2006).

Pd have important roles in photoassimilate translocation from source to sink at the whole plant level. In symplasmic loaders, sucrose produced during photosynthesis in mesophyll cells moves via Pd towards the bundle sheath/phloem parenchyma cells. In apoplastic loaders, such as tobacco and *Arabidopsis*, sucrose from bundle sheath/phloem parenchyma cells is first exported into the apoplast and is then actively loaded into the sieve element–companion cell complex (Lalonde *et al.*, 2004) where Pd are subsequently involved in the transport from the companion cell to the sieve element.

Since AtRGP2:GFP accumulates as a PM peripheral protein within the cytoplasmic sleeve, it may, if overexpressed, result in a modification of the Pd cytoplasmic sleeve, thus altering photoassimilate partitioning and possibly viral spread. Evidence is presented that AtRGP2:GFP overexpression leads to inhibition of photoassimilate export, starch accumulation, stunting of stem elongation, and inhibition of *Tobacco mosaic virus* (TMV) spread. Detailed description of transgenic plants' phenotype is presented and the main morphological and physiological parameters are evaluated.

Materials and methods

Plant material and growth conditions

WT and T_2 *AtRGP2:GFP* homozygous transgenic *Nicotiana tabacum* cv. Samsun (*NN*) were grown either in soil mixed with vermiculite (Pecka Hipper Gan, Rehovot, Israel), or hydroponically with Hoagland's half-strength liquid growth medium (Hoagland and Arnon, 1950) with aeration for 2–3 months. Plants were grown as indicated either in a growth chamber at 25 °C, under long day conditions 16/8 h light/darkness (total light intensity of 80 μE m^{-2} s^{-1}), or in a greenhouse. In the hydroponic experiments, seeds were germinated on sterile agar plates containing 0.44% (w/v) MS (Murashige and Skoog) medium and 1.5% (w/v) sucrose and grown for 2–3 weeks prior to transfer to liquid growth medium. Starch and chlorophyll extraction, callose staining and $^{14}CO_2$ labelling were performed on plants grown in the growth chamber in soil, of comparable physiological age and having the same number of leaves: for starch, chlorophyll, and callose plants had 12–13 leaves [2 months post-germination (mpg) for WT and 2.5 mpg for transgenic plants]; for $^{14}CO_2$ labelling young plants had 9–10 leaves (1.5 mpg WT and 2 mpg transgenic plants), and more mature plants had 13–14 leaves. TMV inoculations were performed on plants grown in the greenhouse, at ~23 °C, under ambient light conditions only (March–April). Upon inoculation, WT and transgenic plants were at a similar physiological age (10–12 leaves). Flowering time and total leaf number on flowering were scored at the moment of flower bud formation for greenhouse plants grown at 25 °C under ambient light conditions.

Morphological parameters measurements

Total root surface area, length, number of tips, and leaf surface area of hydroponically grown plants were determined after scanning the plant organs and analysing the data by WinRHIZO™ software (Arsenault *et al.*, 1995). Dry weight of whole plants and individual leaves was measured after drying the plant material at 80 °C overnight.

Leaf chlorophyll extraction and quantification

Leaf chlorophylls were extracted from two leaf discs, 1.5 cm in diameter, cut from the base and tip-regions of the source and the mid-region of sink leaves from soil-grown plants, by incubating them in 5 ml DMF (*N*,*N*-dimethylformamide, Fluka) for 24 h, in total darkness at room temperature (RT). Chlorophyll *a*, *b*, and total chlorophyll concentrations were calculated according to Moran (1982).

Leaf starch determination

Starch content in leaves was determined by iodine staining: briefly, 4×4 cm leaf sections taken from the base and tip regions of the source and the middle of the sink leaves were excised 1–2 h after the end of the dark period, boiled in 250 ml of 70% (v/v) ethanol for 2–3 min (or until bleaching was complete), washed thoroughly with double distilled water (DDW) and dried at 80 °C for 5–6 h. The dried tissue was then homogenized in 1 ml of 10 mM TRIS buffer (pH 7.4), centrifuged at 5000 rpm for 10 min, and 600 μl of supernatant was mixed with 400 μl of 2% (w/v) I/KI solution and absorbance was measured at 620 nm. A mixture of 600 μl TRIS buffer+400 μl 2% (w/v) I/KI served as a blank. *In situ* starch staining with I/KI was performed according to Rinne *et al.* (2005) except that the stained leaves were incubated in DDW for 5 h to remove excess I/KI before being photographed.

$^{14}CO_2$ labelling

$^{14}CO_2$ labelling of source leaves of young and more mature plants was performed according to Turgeon and Webb (1973) with modifications. Plants were transferred from the growth chamber after 5 h light period (11.00 h) into a laboratory hood with daylight fluorescent illumination of 190 μE m^{-2} s^{-1}. After a 30 min adaptation period, a single source leaf on each plant was enclosed in a transparent polyethylene bag and sealed around the petiole. $^{14}CO_2$ was generated in a 50 ml syringe by the addition of

an excess of 3 M lactic acid to 20 μCi $NaH^{14}CO_3$ (Sigma). The total gas volume was adjusted to 30 cm^3 by pumping air into the syringe. This volume of gas was introduced to six plants (one leaf on each plant): 5 cm^3 for each leaf, resulting in ~3.4 μCi $^{14}CO_2$ per leaf. After 30 min the polyethylene bag was removed. After another 1–30 h (chase period) all the leaves were excised, arranged between Whatman paper, and dried in an oven at 60 °C for 24 h while pressed thin between two metal plates. The dried leaves were exposed to a phosphorimaging plate (Fujifilm) for 1 h at RT and the plate was scanned by Phosphor Imager FLA-5100 (Fujifilm).

Callose staining and quantification

Callose staining and quantification were according to Guenoune-Gelbart *et al.* (2008) with modifications. Whole source and sink leaves from WT and transgenic plants were cut at the petiole, placed immediately in 85% (v/v) ethanol in order to reduce the wounding effect, and incubated in ethanol for 12–15 h at RT with gentle shaking. Sections (3×3 mm) were cut from totally bleached leaf areas lacking large veins, and incubated in a 1% (w/v) aniline blue solution (Fluka) in DDW and 1 M glycine (pH 9.5), at volume ratio of 2:3 for 5 h at RT. Aniline blue fluorescence was viewed and photographed under non-saturating UV conditions using a DMRBE fluorescence light microscope (Leica, Wetzlar, Germany) with a band-pass 340–380 nm excitation filter, an RKP 400 dichromatic mirror, and a long-pass 425 nm emission filter. All measurements were in a linear response range. Image analysis was performed with the IMAGEJ software as described in Levy *et al.* (2007).

Inoculation with TMV

Plants were inoculated with purified TMV particles (stock concentration of 1 mg ml^{-1}) diluted in 0.05 M sodium phosphate buffer (pH 7) to final working concentration of 10 ng ml^{-1} (inoculum). Control (mock) inoculation was made with an equal volume of sodium phosphate buffer alone. No more than four leaves on each plant were inoculated. Four days post-inoculation (4 dpi) infected leaves were harvested, photographed, and the number and diameter of the necrotic lesions were determined. Necrotic lesions substructure was viewed and photographed using a stereoscopic microscope (Zeiss).

Statistical analysis

Statistical analysis of data was performed using JMP6 statistical software (SAS Institute Inc.). Student's each pair *t* test or Tukey–Kramer's all pairs HSD test were performed for statistical significance evaluation of experimental data. In all graphs *y*-axis error bars represent the standard error of the mean values (SEM) as determined by JMP6 software.

Results

Transgenic tobacco expressing Arabidopsis *class 1 reversibly glycosylated polypeptide 2 (^{C1}AtRGP2) has deficiencies in vegetative body development*

Transgenic *Nicotiana tabacum* (cv. Samsun) constitutively expressing the AtRGP2:GFP fusion under the control of CaMV 35S promoter were generated in our laboratory (Sagi *et al.*, 2005) and plants expressing AtRGP2:GFP, were selected from the T_2 generation seeds of independent transgenic lines by germinating them on sterile kanamycin-containing plates. Lines yielding 100% resistant progeny seedlings were assigned as homozygous and three such lines, designated *1-6*, *1-10*, and *12-14*, were used throughout the experiments. All transgenic plants had stable GFP fluorescence at Pd both in source and sink tissues as confirmed by confocal microscopy (see Supplementary Fig. S1 at *JXB* online). Measurements of shoot and root morphological parameters were performed on 10 WT and 20 transgenic plants (10 from line *1-6* and 10 from line *12-14*) grown hydroponically (Fig. 1A). Transgenic plants are stunted and have rosette-like shoots with smaller leaves and poorly developed roots compared with WT plants of the same age (Fig. 1). The biomass of transgenic plants is significantly decreased with plants having shorter stems, smaller and slightly fewer leaves compared with WT plants of the same age (Fig. 2A–D). Total biomass of hydroponically grown 2.5 months post-germination (mpg) transgenic plants is significantly lower than that of WT, being only about 30% of WT biomass on a fresh and dry weight basis (Fig. 2A, B). Furthermore, the biomass distribution in transgenic plants is different from that of WT. In *AtRGP2:GFP* tobacco, 35–40% of total plant biomass is concentrated in leaves, whereas in WT this value is only about 20–25% (Fig. 2A, B). Stem length of transgenic plants is considerably reduced, being about one-fifth of that of WT (Fig. 2D), mainly as a result of shorter internodes (Fig. 1C). The number of leaves of both transgenic lines is lower than WT, but these differences are much less pronounced (Fig. 2C).

Root growth in transgenic plants is also strongly reduced (Figs 1C, 2E–G). Total root length, surface area, and number of tips are significantly lower for both transgenic lines compared to WT (Fig. 2E–G).

Fully expanded source leaves of transgenic plants are chlorotic and smaller in size and weight than corresponding leaves of WT plants (Figs 1B, 3A, C, E). Chlorotic leaves seem to be thicker, less flexible and are more robust than the corresponding WT leaves. This phenomenon is expressed in leaf specific weights: the ratio of leaf fresh or dry weight to its surface area. There are significant differences in the pattern of change in leaf specific weight during maturation between WT and transgenic plants (Fig. 3B, D). Specific fresh weight (SFW) of leaves increases with the size and age both in transgenic and WT plants, but in transgenic plants, mature leaves exhibit significantly higher SFW than younger ones (Fig. 3B). Conversely, specific dry weight (SDW) of leaves slightly decreases as the leaf matures due to the relative increase in water content as cells expand during leaf growth (Fig. 3D 'WT'). However, the SDW of fully expanded leaves in both transgenic lines is significantly higher than that of younger expanding leaves (Fig. 3D). For young, expanding, non-chlorotic leaves of transgenic plants, both SFW and SDW do not significantly differ from those of WT (Fig. 3B, D), although absolute values of leaf weight and area are lower than in WT (Fig. 3A, C, E).

Flowering time of transgenic plants is 1.5–2 times longer than that of WT. WT plants grown both in the greenhouse and in the growth chamber start to flower, on average, 2.5–3 mpg. Transgenic lines grown under identical conditions flower about 2 months later (Fig. 4A, B), initiate flowering at about 5 mpg, and develop long determinate

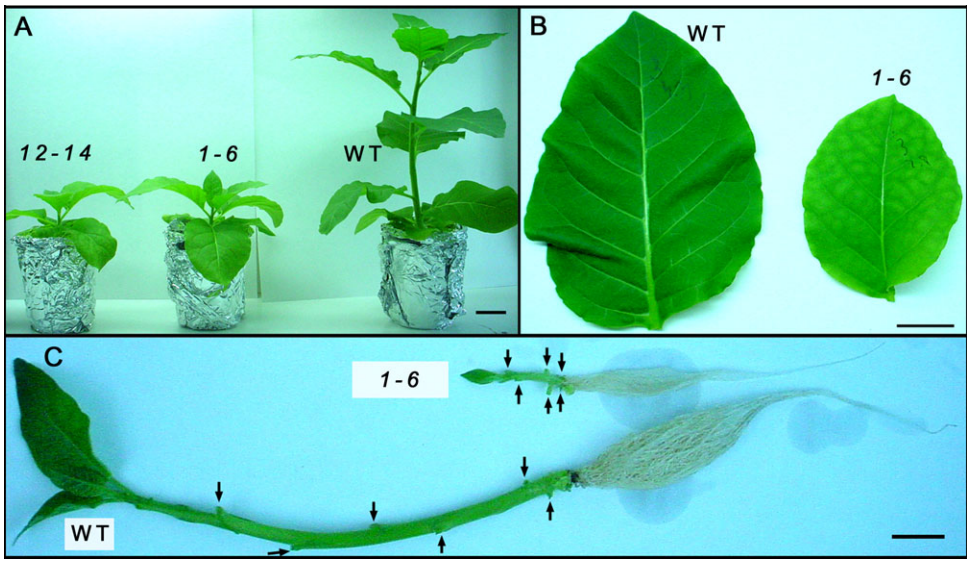

Fig. 1. Effect of overexpression of *AtRGP2:GFP* on the morphology of hydroponically grown tobacco plants. (A) Two independent transgenic lines, *1-6* and *12-14*, and WT at 2.5 mpg are shown: transgenic plants have rosette-like shoots, smaller leaves, and chlorosis in the source leaves. (B) Fully developed corresponding leaves (5th or 6th from the base) from individual WT and transgenic plant (line *1-6*). The transgenic leaf is chlorotic and smaller in size than WT. (C) Stem and root of WT and transgenic plants from line *1-6*. Leaves were excised to expose the nodes (arrows). The internodes of the transgenic stem are much shorter and its roots are less well developed. Bar, 5 cm (A); 3 cm (B, C).

stem with normally looking inflorescences (Fig. 4B). The number of leaves of both transgenic lines at flowering time is higher than WT (Fig. 4C).

During sink-to-source transition, transgenic leaves accumulate starch and undergo chlorosis

Leaf chlorosis initially appears at the tip region and in fully expanded leaves it extends to the entire leaf (Fig. 5A). Leaf starch and total chlorophyll levels of *AtRGP2:GFP* transgenic and WT plants grown in the growth chamber were determined from sections of tip and base of source leaves (5th or 6th from the base) and from sections taken from the centre of sink leaves (10th or 11th from the base) (Fig. 5A). Chlorotic source leaves of transgenic plants accumulate 6–8 times higher starch levels, especially in the tip region, compared with sink leaves (Fig. 5B). This is inversely correlated with chlorophyll levels of the same region (Fig. 5C). However, in WT plants there are no differences in starch and chlorophyll content between source and sink leaves or between tip and base regions of source leaves (Fig. 5B, C). Both transgenic lines have similar levels of starch and chlorophyll content between 'source-leaf' base region and 'sink-leaves' (Fig. 5B, C). The I/KI stained fully expanded chlorotic source leaf of transgenic plant shows very high levels of starch in the leaf tip region (Fig. 6C). In WT leaves only traces of transient starch are detectable (Fig. 6C). These results suggest that high specific dry weight of source leaves of *AtRGP2:GFP* plants could be caused by excessive starch accumulation in those leaves, and the chlorotic phenotype is probably due to less chlorophyll.

Distribution of radioactivity after $^{14}CO_2$ pulse labelling

Source leaf chlorosis and starch accumulation in *AtRGP2:GFP* plants might be a result of an inhibition in symplasmic transport of photoassimilate between and from mesophyll cells towards the phloem, followed by excessive starch accumulation in mesophyll tissue. To test this assumption $^{14}CO_2$ loading experiments were carried out with first fully expanded source leaf (7th from the tip, when the smallest visible leaf counted as 1) of WT and transgenic plants (line *12-14*). At the time of labelling the leaf of the transgenic plant exhibited weak signs of chlorosis. Following a 30 min pulse the plants were allowed to translocate fixed [^{14}C]-photosynthate for 1–30 h (chase time). Autoradiographs of importing leaves (above the labelled leaf) after a 1 h translocation period show that less amount of [^{14}C]-photosynthate is translocated in transgenic plants compared to WT (Fig. 6A). However, no significant differences are seen in the pattern of radioactivity distribution among the ^{14}C importing leaves between WT and *AtRGP2:GFP* plants (Fig. 6A). Since, in tobacco, phloem transport takes place preferentially along the orthostichies (Jones *et al.*, 1959) only leaves located above the labelled leaf produce a maximum signal (Fig. 6A). Autoradiographs of labelled WT leaves after 30 h translocation time show that most of the fixed [^{14}C]-photosynthate has been loaded and exported out of the leaf, since the highest radioactivity is retained in the major veins and much less in the minor veins and mesophyll (Fig. 6B). However, in the transgenic leaf, the radioactivity is distributed unevenly, with leaf base and tip regions retaining most of the signal, which is concentrated in the form of patches in the interveinal areas (Fig. 6B). The pattern of radioactivity distribution in the tip

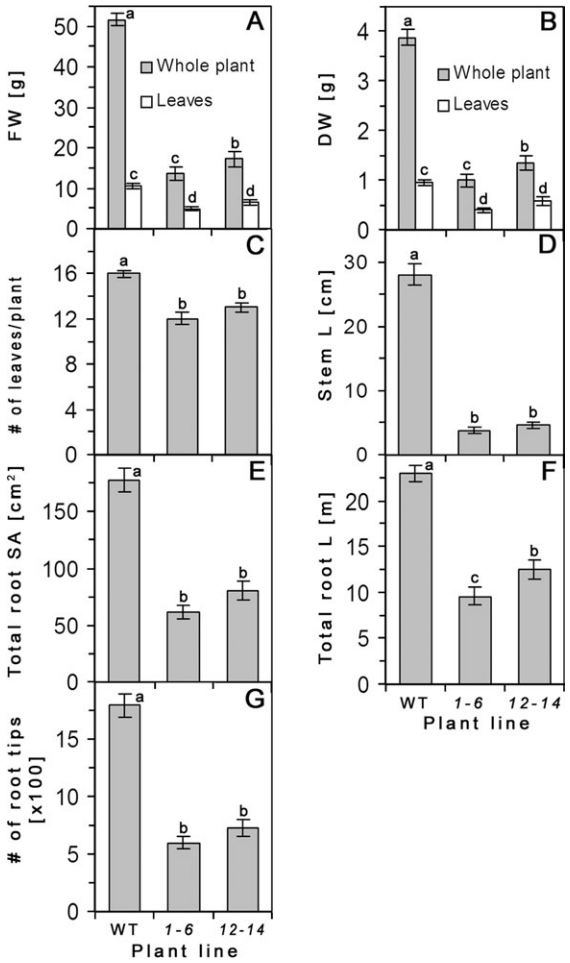

Fig. 2. Shoot and root morphological parameters of two independent *AtRGP2:GFP* transgenic lines (*1-6* and *12-14*) and of WT, hydroponically grown tobacco at 2.5 mpg (12–16 leaves). The total fresh (A) and dry (B) biomass of the whole plant and of detached leaves, the number of plant leaves (C), the stem length (D), the total root surface area (E), the total root length (F), and the number of root tips (G) are all lower for both transgenic lines compared to WT control. Values represent means ±SE of 10 individual plants per line. Lowercase letters indicate statistical differences at $P < 0.0001$ as determined by Student's *t* test.

region of the transgenic leaf resembles that of starch accumulation which is also in the interveinal areas (Fig. 6C). These results indicate that starch accumulation and subsequent growth deficiency of *AtRGP2:GFP* plants result from the retention of photoassimilate in source leaves, which limits their loading to the phloem and translocation to sink tissues.

Excessive plasmodesmal callose accumulation

Starch accumulation in the source leaves of *AtRGP2:GFP* transgenic plants may be the result of decreased sugar transport out of the source leaves. Callose deposition and degradation in the cell walls around Pd is one of the physiological mechanisms regulating Pd permeability. The hypothesis that, in *AtRGP2:GFP* transgenic plants, the growth deficiency and starch accumulation observed in source leaves could be a result of decreased Pd conductivity due to excessive callose accumulation was checked. Callose levels associated with Pd were determined by aniline blue staining (Baluska *et al.*, 1999; Bayer *et al.*, 2004; Sagi *et al.*, 2005; Levy *et al.*, 2007; Guenoune-Gelbart *et al.*, 2008). In order to avoid wound-induced callose accumulation that occurs on cutting a leaf, sink and source leaves were removed at the base of the petiole and immediately soaked and fixed in 85% (v/v) ethanol prior to aniline blue staining (Fig. 7A–D). Transgenic plants have significantly higher callose associated with Pd in source leaves compared to WT (Fig. 7E).

Control experiments determined that there was no bleed-through between GFP and aniline channels (this work; Sagi *et al.*, 2005; Levy *et al.*, 2007) (data not shown), thereby ruling out the possibility that plasmodesmal AtRGP2:GFP fluorescence contributes to measured callose fluorescence intensity. Moreover, under our experimental conditions no GFP fluorescence was detected in ethanol-fixed leaf tissue when viewed under optical configuration of GFP (data not shown). Therefore fluorescence measured in aniline blue-stained *AtRGP2:GFP* tobacco leaf epidermal cells is due exclusively to callose. In non-fixed leaves, GFP fluorescence is unaffected by aniline blue staining (Sagi *et al.*, 2005).

Inhibition of cell-to-cell spread of virus

The above data suggest that AtRGP2:GFP overexpression may directly or indirectly block Pd. This hypothesis predicts that virus spread would be impaired in transgenic plants. WT (at 2 mpg) and transgenic plants (at 2.5 mpg) were inoculated with purified TMV particles. Leaf pairs 3–4, 5–6, or 7–8 (counted from the base) were chosen for inoculation. Measurements however, were performed only with leaves 5–6, which were similar in size between WT and transgenic plants used in this experiment. At 4 dpi, necrotic lesions are clearly seen both on WT and transgenic plants (Fig. 8B, C), and are absent from mock inoculated plants (Fig. 8A). The number of lesions per leaf on WT is significantly higher than on transgenic plants (Fig. 8D). The shape and size of the lesions also differ between WT and transgenic plants (Fig. 8E–G). Lesions on WT leaves are round with clear margins, and three distinct regions could be discerned: a central dark green (chlorophyll concentration), a middle necrotic ring, and an outer chlorotic ring (Fig. 8F). Lesions on both transgenic lines are smaller in size than in WT, and have an irregular shape with unclear diffuse margins and appear as simple necrotic spots (Fig. 8E). Measurements of lesion diameter showed that the necrotic lesions on WT plants are significantly bigger than on both transgenic lines (Fig. 8G).

The data showing a decreased number of necrotic lesions per leaf and the decreased size of the lesions suggests that expression of AtRGP2:GFP in some manner impairs initial virus spread.

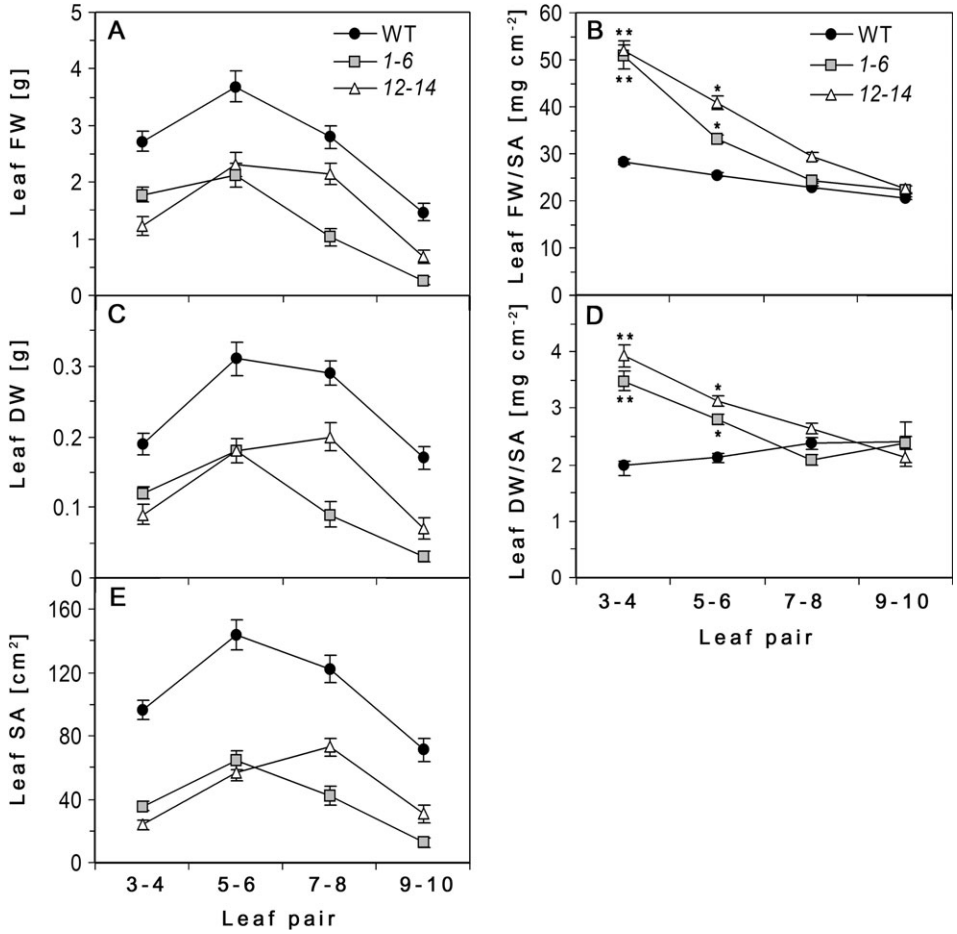

Fig. 3. Comparison of leaf physical parameters along the growth axis. Fresh (A) and dry (C) weights and surface area (E) of leaf pairs 3–4, 5–6, 7–8, and 9–10 counted from the base. Leaf specific fresh weight (B) and specific dry weight (D) is expressed as the ratio of leaf weight to surface area (SA). Values represent the average between pairs of leaves of hydroponically grown *AtRGP2:GFP* transgenic lines (*1-6* and *12-14*) and WT tobacco at 2.5 mpg as means ±SE of 10 individual plants per line. Asterisks in (B) and (D) indicate statistical differences between the leaves within the transgenic lines and between leaves of transgenic and WT at $P \leqslant 0.0001$–0.0091 as determined by Student's *t* test.

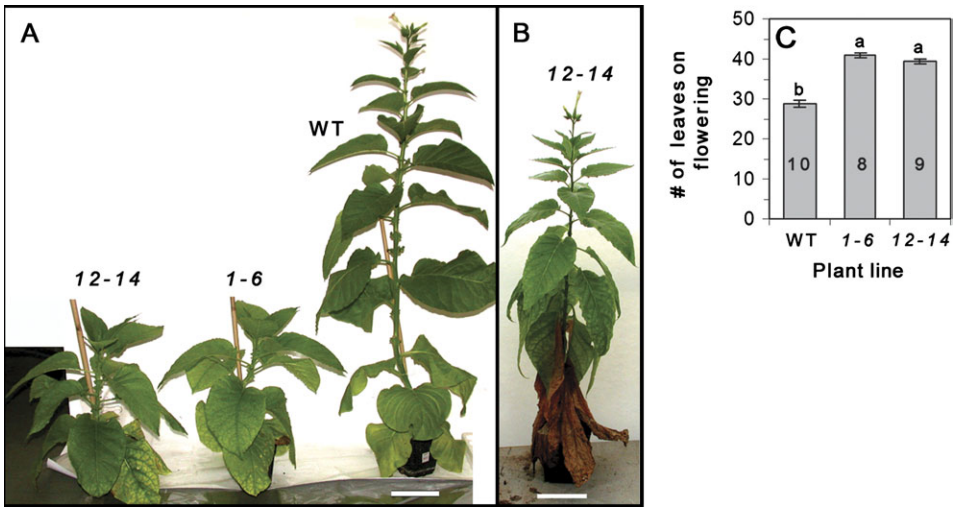

Fig. 4. (A) WT plants start flowering at 2.5 mpg, while both transgenic lines remain vegetative. (B) Transgenic plant from line *12-14*, only starts flowering at 5 mpg. (C) Total number of leaves (including the dead ones) per plant at the moment of flowering bud formation. Values represent means ±SE of 8–10 individual plants (*n*, shown within columns in C). Lowercase letters indicate statistical differences at $P < 0.0001$ as determined by Student's *t* test. Bar=10 cm (A, C).

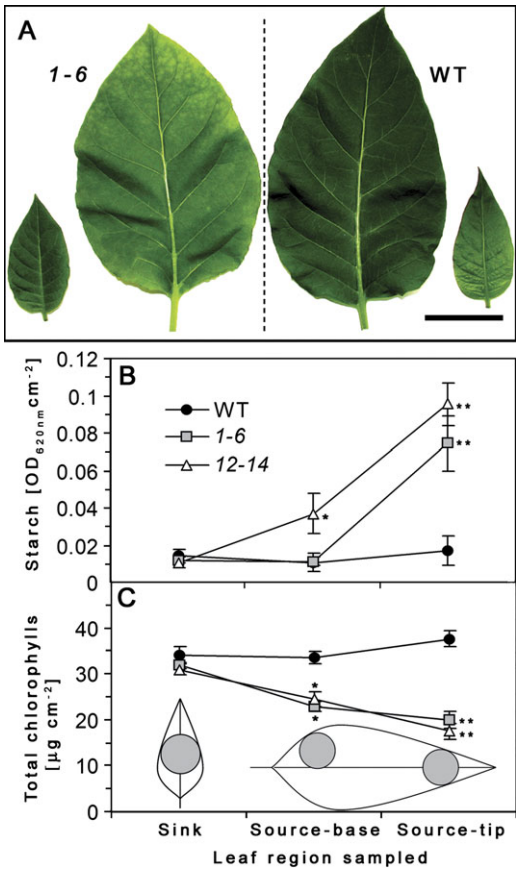

Fig. 5. Leaf starch (B) and chlorophyll content (C) of *AtRGP2:GFP* and WT tobacco. (A) Sink leaf (9th or 10th from the base) and source leaf (5th or 6th from the base) of transgenic line *1-6* (left) and of WT (right). Leaf tissue was sampled from leaf discs as shown in (C). Leaf starch content was determined from leaf tissue homogenate stained with I/KI. Total leaf chlorophyll content was determined by the absorption of chlorophyll pigments extracted by DMF. Values represent means ±SE of a pool of comparable leaves of five individual plants from each line (B, n=10–15; C, n=7–12). Asterisks in (B) and (C) indicate statistical differences at P <0.0001 as determined by Student's t test. Bar=5 cm (A).

Discussion

Homozygous transgenic tobacco plants constitutively expressing plasmodesmal AtRGP2:GFP exhibit stunted rosette-like growth, high callose accumulation around Pd, high starch accumulation, chlorosis in the source leaves, and delayed flowering. This phenotype is more extreme in homozygous than in heterozygous lines (not shown). TMV spread is also impaired. These pleiotropic effects are probably due to a partial blocking of cell-to-cell transport and export from source to sink either as a result of AtRGP2:GFP accumulation in the Pd and/or the increased callose accumulation around Pd.

A striking feature of *AtRGP2:GFP* tobacco is the strong chlorosis and starch accumulation in the source leaves (Figs 5, 6C). The dynamic pattern of starch accumulation and chlorophyll degradation in transgenic source leaves is basipetal (Figs 5, 6C) and is reminiscent of the pattern of sink-to-source transition in a maturing leaf which is also basipetal, where the basal part of the leaf undergoes sink-to-source transition later than the tip. This pattern suggests that, as a region becomes a source, its capacity to export sugars is blocked, leading to starch accumulation and chlorosis (Figs 5, 6C). $^{14}CO_2$ pulse labelling demonstrates that, in transgenic plants, the loading of photoassimilate to the phloem is inhibited, as most of the fixed ^{14}C is retained in the interveinal areas (probably mesophyll) of source leaves in a pattern that is similar to starch accumulation (Fig. 6B). In view of these results, it is proposed that in *AtRGP2:GFP* tobacco, the blockage of Pd in the mesophyll tissue and/or in the phloem (between companion cells and sieve elements) leads to a build-up of sucrose and starch accumulation in mesophyll cells. In plants that exhibit a severe rosette-like growth pattern, chlorosis is observed both in sink and source leaves (data not shown). This may be attributed to variable transgene expression levels which were not determined in this study.

It has been proposed that RGP may be involved in the biosynthesis of polysaccharides such as, cellulose, hemicellulose and/or starch (Dhugga *et al.*, 1997; Langeveld *et al.*, 2002). Thus, it might be argued that, in transgenic plants, the overexpression of AtRGP2:GFP may lead to increased wall polysaccharides resulting in a mass addition to leaf tissues. However, since sink leaves of *AtRGP2:GFP* plants show little or no difference in specific weight from WT (Fig. 3), and also no chlorosis or starch accumulation (Fig. 5), it is suggested that it is the symplasmic block in source leaves with the consequent starch accumulation that is the main reason of elevated source leaf specific weight. The reduction in root growth is also consistent with the proposed block in symplasmic transport (Fig. 2E–G). Langeveld *et al.* (2002) reported that transgenic tobacco plants constitutively expressing wheat *RGP1* or *RGP2* (which share 70% sequence similarity with *Arabidopsis* RGP2) show no differences from WT in development, growth rate, and size and shape of starch granules in the chloroplasts. Their data, however, was obtained with heterozygous lines and as we previously stated, in heterozygous lines phenotypic differences are minor.

In day-neutral tobacco, flowering is controlled, in part, by the level of the floral stimulus exported from mature, expanded leaves to the shoot apical meristem (McDaniel, 1996). The flowering time of *AtRGP2:GFP* tobacco is nearly 1.5 times longer than that of WT (Fig. 4). This might be due to a reduced transport of floral stimulus from the source leaves to the apical meristem as a result of Pd blockage or a combination of reduced source leaf size (Fig. 3) and decreased Pd permeability.

Viral movement proteins (MPs) that target to Pd are known to facilitate the cell-to-cell spread of viruses in plants. A number of studies have shown that constitutive expression of viral Pd-associated movement proteins in transgenic plants leads to the physiological and developmental aberrations resembling those which appear during compatible viral infection (Balachandran *et al.*, 1995;

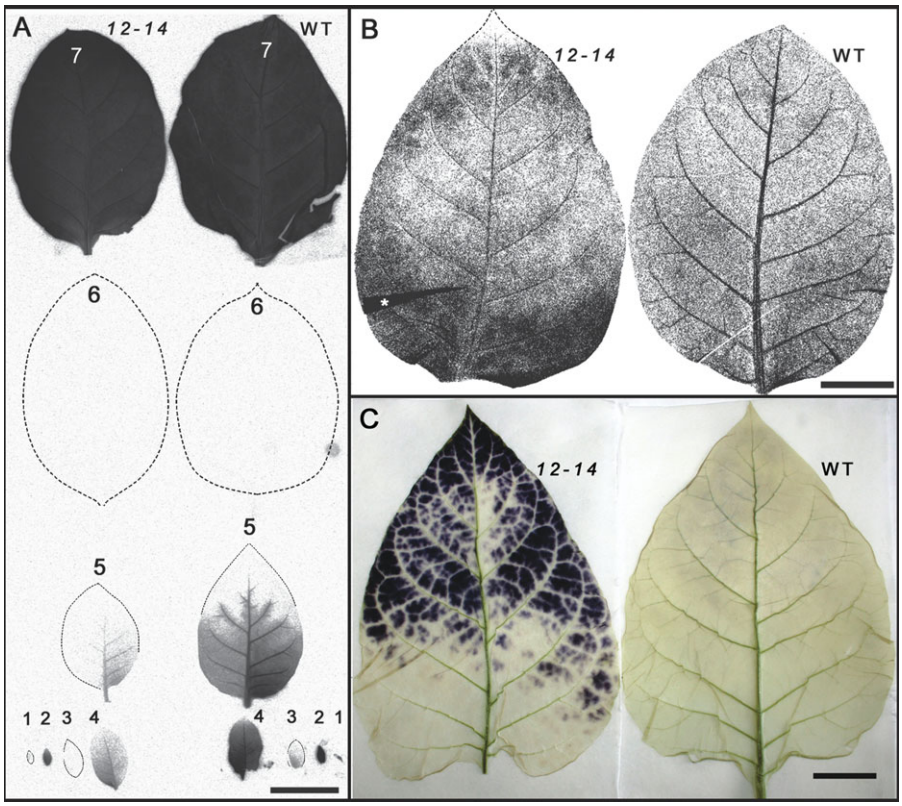

Fig. 6. ^{14}C distribution pattern after 30 min $^{14}CO_2$ pulse labelling, and starch accumulation pattern in *AtRGP2:GFP* (line *12-14*) and WT tobacco leaves. (A) Autoradiograph of labelled fully expanded source (no. 7) and importing (no. 1 to no. 5) leaves of young transgenic and WT plants (both having 9–10 leaves) after 1 h chase. Sink leaves of transgenic plant import less [^{14}C]-photosynthate than corresponding WT leaves after the 1 h translocation period, although the pattern of radioactivity distribution is similar. Lower leaves (nos 8–10) did not accumulate detectable radioactivity after 1 h chase time (not shown). (B) Autoradiograph of $^{14}CO_2$ labelled fully expanded source leaves (7th from the tip) of more mature plants (13–14 leaves) after 30 h chase. The radioactivity in the WT leaf is mostly concentrated in major veins, while the transgenic leaf has higher radioactivity in interveinal (mesophyll) areas especially at the tip and the base. (C) Starch accumulation pattern in WT and chlorotic transgenic, fully expanded source leaf. After 5 h washing of I/KI-stained leaves large amounts of starch remain at the leaf tip region of transgenic plant, while almost no starch is detectable in WT leaf. (A, B) Representative pictures of two (A) and three (B) independent experiments each with three WT and three transgenic plants. Leaf fold area in (B) is marked by an asterisk. Bar=3 cm (A, B, C).

Almon *et al.*, 1997; Herbers *et al.*, 1997, 2000; Hofius *et al.*, 2001; Rinne *et al.*, 2005; Biemelt and Sonnewald, 2006; Kronberg *et al.*, 2007). A similar phenotype as observed for *AtRGP2:GFP* transgenic tobacco was observed in potato constitutively expressing ^{TMV}MP (Olesinski *et al.*, 1996), in tobacco constitutively expressing ^{TSWV}MP (Rinne *et al.*, 2005), and in *Arabidopsis* plants constitutively expressing high levels of ^{PLRV}MP (Kronberg *et al.*, 2007). ^{TMV}MP transgenic potato plants had reduced sugars export and sink deficiency, except when the transgenic plants possessed tubers and flowers (Olesinski *et al.*, 1996). During vegetative growth of transgenic *Arabidopsis* plants expressing high levels of ^{PLRV}MP, carbohydrate export is blocked as evident by starch accumulation in source leaves and reduced growth. At later stages of plant development, this block is released, resulting in a higher seed yield of transgenic plants. The abolition of the carbohydrate export block is paralleled by a reduced association of ^{PLRV}MP with Pd (Kronberg *et al.*, 2007). During floral induction, the increase in Pd conductivity may have been controlled by developmental signals specific to this state (Kobayashi *et al.*, 2005). It is possible that in *AtRGP2:GFP* transgenic tobacco, as in MP transgenic plants, such signals up-regulate Pd permeability during flowering and storage organ development and help to overcome the negative effect of the transgene.

AtRGP2:GFP accumulation leads to plasmodesmal callose deposition

In *AtRGP2:GFP* transgenic plants, there is increased callose accumulation around Pd in both sink and source leaves, with significantly higher levels in source leaves than in sink (Fig. 7). Transgenic tobacco plants expressing ^{TSWV}MP, like *AtRGP2:GFP* plants, accumulate increased levels of callose at Pd of source leaves, are stunted, and accumulate increased levels of starch when grown at 22 °C (Rinne *et al.*, 2005). When grown at higher temperature (32 °C) this phenotype is complemented, due to a reduction in callose levels. It was proposed that the excessive callose accumulation around Pd blocks symplasmic sucrose transport resulting in the

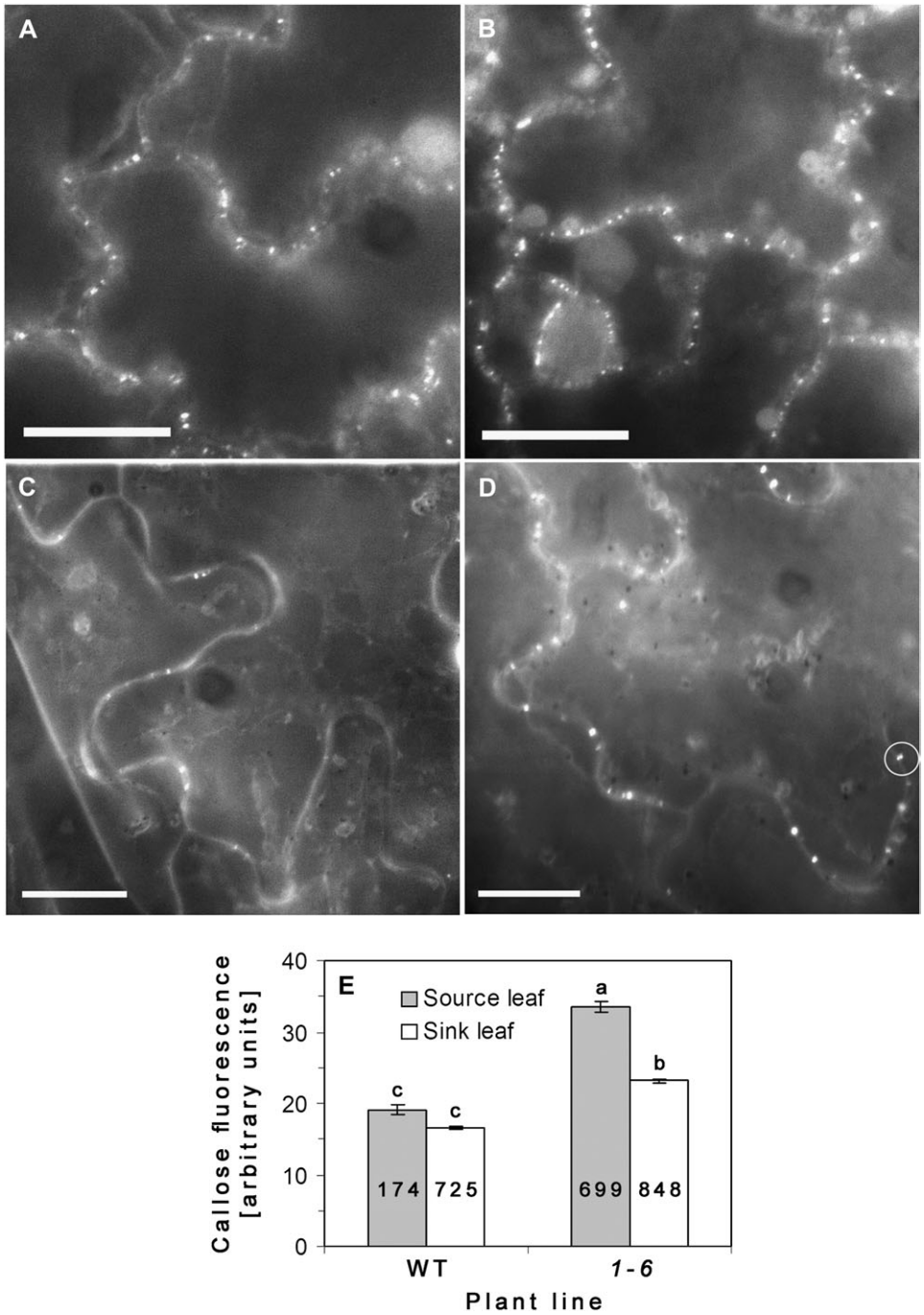

Fig. 7. Basal callose levels in source (5th or 6th from the base) and sink (9th or 10th from the base) leaves of *AtRGP2:GFP* transgenic and WT plants. (A–D) Fluorescent micrographs of aniline blue-stained leaf epidermal cells of WT sink (A), transgenic sink (B), WT source (C), and transgenic source (D) leaves. (E) Fluorescence intensity (arbitrary units) of callose deposits, measured from randomly chosen cells, determined by subtracting background intensity from the maximal intensity value within a defined area enclosing Pd foci (white circle in D). Note: in WT source leaves much fewer Pd are stained with aniline blue than in transgenic leaves. Values in (E) represent means ±SE of Pd callose intensity of three leaves taken from two individual plants of each line. Lowercase letters indicate statistical differences at $P < 0.05$ as determined by the Tukey–Kramer HSD test. Numbers within columns indicate the number of fluorescent foci examined (*n*). Bar=20 μm (A–D).

accumulation of starch in mesophyll cells and in growth retardation of ^{TSWV}MP transgenic plants (Rinne *et al.*, 2005). It is hypothesized that high plasmodesmal callose levels in *AtRGP2:GFP* tobacco may similarly contribute to the observed phenotype by reducing Pd permeability, with a consequential reduction in symplasmic transport of photoassimilate. In addition, the increased levels of AtRGP2:GFP fusion in Pd may also cause Pd occlusion. Since RGP proteins were shown to form large homo-multimeric complexes of ~400 kDa (Dhugga, 2006; De Pino *et al.*, 2007) it is

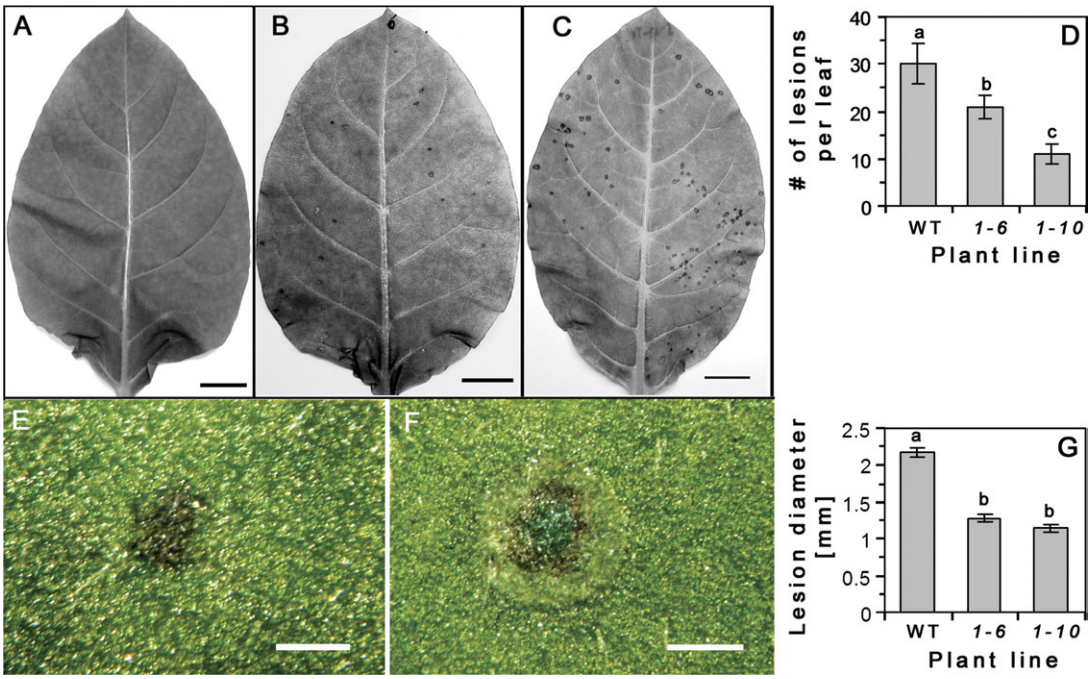

Fig. 8. Source leaves of *AtRGP2:GFP* transgenic and WT tobacco plants inoculated with TMV, at 4 dpi. Dry lesions are present on representative leaves (5th or 6th from the base): transgenic line *1-6*, mock inoculated (A) and virus-inoculated (B); and WT, virus-inoculated (C). The number of lesions is lower on transgenic leaves than on WT (D). (E, F) Characteristics of representative lesions from transgenic line *1-6* (E) and WT (F) on 4 dpi as viewed from the adaxial surface. Lesions on transgenic plants have an irregular shape, lack a chlorotic ring and central chlorophyll concentration (E), and are smaller in size than WT (G). Lesions on WT leaf are regular round-shaped, have three distinctive regions: chlorotic and necrotic rings and central chlorophyll concentration (F). Values represent: in (D), means ±SE of average of two leaves per plant, from 13 WT and 16 transgenic (8 from each line) individual plants; in (G), means ±SE of lesion diameter (n=32–41) of randomly chosen infected leaves. Lowercase letters in (D) and (G) indicate statistical differences at P <0.05 in (D), and at P <0.0001 in (G), as determined by Student's t test. Bar=2 cm (A–C); 1 mm (E, F).

probable that the accumulation of the overexpressed complex in the cytoplasmic sleeve of Pd could lead to lower Pd conductivity. Such blockage would possibly be both at the level of cell-to-cell transport and at the symplasmic level by blockage of transport during phloem loading in the source tissue or at the level of unloading in the sink tissue. Reduction in Pd permeability is also expressed in an inhibition of the initial cell-to-cell spread of TMV (Fig. 8).

Another possibility is that AtRGP2 is more directly involved in callose biosynthesis in cell walls around Pd. It was previously hypothesized that RGP proteins are involved in the biosynthesis of plant cell wall polysaccharides (Dhugga *et al.*, 1997). However, an analysis of *Arabidopsis rgp1* and *rgp2* knockout mutants showed that these proteins probably do not play an essential role in callose biosynthesis (Drakakaki *et al.*, 2006). It was suggested that RGP1 and RGP2 may possibly be involved in cell division, since both proteins localize to cytoplasm and Golgi vesicles in actively growing tissues (Drakakaki *et al.*, 2006). The importance of RGPs in cell wall deposition during cell division and growth is consistent with our observation of AtRGP2:GFP also being highly enriched in dividing cells of the shoot apical meristem of transgenic plants where it strongly marks the forming cell plate along with developing Pd (see Supplementary data at *JXB* online).

Impairment of viral cell-to-cell spread

Our results using *N. tabacum* cv. Samsun (*NN*) expressing AtRGP2:GFP indicate that cell-to-cell spread of TMV is reduced in *AtRGP2:GFP* plants (Fig. 8). Normally in *N. tabacum* (*NN*), TMV infection and spread induce a hypersensitive response (HR) resulting in the formation of necrotic lesions. The HR reaction is induced as the virus replicates and spreads from an initially infected cell to a limited number of surrounding cells. Viral spread is limited by the HR and resulting cell death and the formation of a necrotic lesion (Hull, 2002). If the virus cannot spread, no visible necrotic lesions are formed (Hull, 2002). In *AtRGP2:GFP* plants, the number of lesions compared to WT is smaller and the lesions that form are smaller and lack the characteristic chlorotic ring seen in the WT control (Fig. 8). It is suggested that AtRGP2:GFP overexpression blocks virus spread either directly by physically blocking the plasmodesmata or indirectly by stimulating callose accumulation either by increasing callose synthesis or by inhibiting callose hydrolysis, both of which would close Pd.

Conclusion

Pd conductivity is a dynamic parameter which is often affected during developmental transitions and by various

biotic and abiotic factors (Crawford and Zambryski, 2001; Liarzi and Epel, 2005). Reduction in Pd permeability caused either by alteration of their protein composition (AtRGP2:GFP accumulation) or by secondary processes triggered by such alteration (e.g. callose deposition) may block the symplasmic translocation from the source to the sink and result in considerable deficiencies in plant growth and development. These observations suggest that overexpression of plasmodesmal proteins could result in a subsequent cell-to-cell transport block and could also result in evoking the plant defence response resulting in callose deposition leading to inhibition of photosynthate translocation and viral spread. Based on these results, it is suggested that some of the symptoms displayed by virus-infected plants may be due to a partial blocking of Pd as a result of viral infection.

Supplementary data

Supplementary data can be found at *JXB* online.

Supplementary Fig. S1. Confocal micrographs of AtRGP2:GFP localization in shoot apical meristem, and in sink and source leaf epidermis of 35S::*AtRGP2:GPF* transgenic tobacco.

Supplementary Video S1. Time series of tobacco shoot apical meristem section showing AtRGP2:GFP in Golgi vesicles.

Acknowledgements

We thank Amram Eshel (TAU) for use of the WinRHIZO facility and assistance in $^{14}CO_2$ labelling experiments; and Amit Levy (TAU) for help in the callose staining and measurement procedure. This research was supported in part by Resource Grant Award IS-3222-01C from the US–Israel Binational Agricultural Research and Development Fund, by the Israel Science Foundation (Grant 723/00-17.1), and by the Manna Institute for Plant Biosciences at Tel Aviv University.

References

Almon E, Horowitz M, Wang HL, Lucas WJ, Zamski E, Wolf S. 1997. Phloem-specific expression of the *Tobacco mosaic virus* movement protein alters carbon metabolism and partitioning in transgenic potato plants. *Plant Physiology* **115,** 1599–1607.

Arsenault JL, Pouleur S, Messier C, Guay R. 1995. WinRHIZO(TM), a root-measuring system with a unique overlap correction method. *HortScience* **30,** 906.

Balachandran S, Hull RJ, Vaadia Y, Wolf S, Lucas WJ. 1995. Alteration in carbon partitioning induced by the movement protein of *Tobacco mosaic virus* originates in the mesophyll and is independent of change in the plasmodesmal size exclusion limit. *Plant, Cell and Environment* **18,** 1301–1310.

Baluska F, Samaj J, Napier R, Volkmann D. 1999. Maize calreticulin localizes preferentially to plasmodesmata in root apex. *The Plant Journal* **19,** 481–488.

Bayer E, Thomas CL, Maule AJ. 2004. Plasmodesmata in *Arabidopsis thaliana* suspension cells. *Protoplasma* **223,** 93–102.

Biemelt S, Sonnewald U. 2006. Plant–microbe interactions to probe regulation of plant carbon metabolism. *Journal of Plant Physiology* **163,** 307–318.

Crawford KM, Zambryski PC. 2001. Non-targeted and targeted protein movement through plasmodesmata in leaves in different developmental and physiological states. *Plant Physiology* **125,** 1802–1812.

De Pino V, Boran M, Norambuena L, Gonzalez M, Reyes F, Orellana A, Moreno S. 2007. Complex formation regulates the glycosylation of the reversibly glycosylated polypeptide. *Planta* **226,** 335–345.

Delgado IJ, Wang ZH, de Rocher A, Keegstra K, Raikhel NV. 1998. Cloning and characterization of AtRGP1: a reversibly autoglycosylated Arabidopsis protein implicated in cell wall biosynthesis. *Plant Physiology* **116,** 1339–1349.

Dhugga KS. 2006. Golgi glucan synthases. In: Hayashi T, ed. *The science and lore of the plant cell wall: biosynthesis, structure and function*. Boca Raton: BrownWalker Press, 114–122.

Dhugga KS, Tiwari SC, Ray PM. 1997. A reversibly glycosylated polypeptide (RGP1) possibly involved in plant cell wall synthesis: purification, gene cloning, and trans-Golgi localization. *Proceedings of the National Academy of Sciences, USA* **94,** 7679–7684.

Dhugga KS, Ulvskov P, Gallagher SR, Ray PM. 1991. Plant polypeptides reversibly glycosylated by UDP-glucose. Possible components of Golgi beta-glucan synthase in pea cells. *Journal of Biological Chemistry* **266,** 21977–21984.

Drakakaki G, Zabotina O, Delgado I, Robert S, Keegstra K, Raikhel N. 2006. Arabidopsis reversibly glycosylated polypeptides 1 and 2 are essential for pollen development. *Plant Physiology* **142,** 1480–1492.

Epel BL, Kuchuck B, Kotlizky G, Shurtz S, Erlanger M, Yahalom A. 1995. Isolation and characterization of plasmodesmata. *Methods in Cell Biology* **50,** 237–253.

Epel BL, van Lent JWM, Cohen L, Kotlizky G, Katz A, Yahalom A. 1996. A 41 kDa protein isolated from maize mesocotyl cell walls immunolocalizes to plasmodesmata. *Protoplasma* **191,** 70–78.

Faulkner CR, Blackman LM, Cordwell SJ, Overall RL. 2005. Proteomic identification of putative plasmodesmatal proteins from *Chara corallina*. *Proteomics* **5,** 2866–2875.

Guenoune-Gelbart D, Elbaum M, Sagi G, Levy A, Epel BL. 2008. *Tobacco mosaic virus* (TMV) replicase and movement protein function synergistically in facilitating TMV spread by lateral diffusion in the plasmodesmal desmotubule of *Nicotiana benthamiana*. *Molecular Plant–Microbe Interactions* **21,** 335–345.

Heinlein M, Epel BL. 2004. Macromolecular transport and signalling through plasmodesmata. *International Review of Cytology* **235,** 93–164.

Herbers K, Tacke E, Hazirezaei M, Krause KP, Melzer M, Rohde W, Sonnewald U. 1997. Expression of a luteoviral movement protein in transgenic plants leads to carbohydrate accumulation and reduced photosynthetic capacity in source leaves. *The Plant Journal* **12,** 1045–1056.

Herbers K, Takahata Y, Melzer M, Mock HP, Hajirezaei M, Sonnewald H. 2000. Regulation of carbohydrate partitioning during the interaction of *Potato virus Y* with tobacco. *Molecular Plant Pathology* **1,** 51–59.

Hoagland DR, Arnon DI. 1950. The water-culture method of growing plants without soil. *California Agricultural Experiment Station Circular* **347**.

Hofius D, Herbers K, Melzer M, Omid A, Tacke E, Wolf S, Sonnewald U. 2001. Evidence for expression level-dependent modulation of carbohydrate status and viral resistance by the *Potato leaf roll virus* movement protein in transgenic tobacco plants. *The Plant Journal* **28,** 529–543.

Hull R. 2002. *Matthews' plant virology*: Academic Press.

Jones H, Martin RV, Porter HK. 1959. Translocation of ^{14}carbon in tobacco following assimilation of ^{14}carbon dioxide by a single leaf. *Annals of Botany* **23,** 493–508.

Kobayashi K, Kim I, Cho E, Zambryski P. 2005. Plasmodesmata and plant morphogenesis. In: Oparka KJ, ed. *Plasmodesmata.* Annual Plant Reviews, Vol. 18. Oxford: Blackwell Publishing, 90–112.

Kronberg K, Vogel F, Rutten T, Hajirezaei MR, Sonnewald U, Hofius D. 2007. The silver lining of a viral agent: increasing seed yield and harvest index in Arabidopsis by ectopic expression of the *Potato leaf roll virus* movement protein. *Plant Physiology* **145,** 905–918.

Lalonde S, Wipf D, Frommer WB. 2004. Transport mechanisms for organic forms of carbon and nitrogen between source and sink. *Annual Review of Plant Biology* **55,** 341–372.

Langeveld SM, Vennik M, Kottenhagen M, Van Wijk R, Buijk A, Kijne JW, de Pater S. 2002. Glucosylation activity and complex formation of two classes of reversibly glycosylated polypeptides. *Plant Physiology* **129,** 278–289.

Lee JY, Taoka K, Yoo BC, Ben-Nissan G, Kim DJ, Lucas WJ. 2005. Plasmodesmal-associated protein kinase in tobacco and Arabidopsis recognizes a subset of non-cell-autonomous proteins. *The Plant Cell* **17,** 2817–2831.

Levy A, Erlanger M, Rosenthal M, Epel BL. 2007. A plasmodesmata-associated beta-1,3-glucanase in Arabidopsis. *The Plant Journal* **49,** 669–682.

Liarzi O, Epel BL. 2005. Development of a quantitative tool for measuring changes in the coefficient of conductivity of plasmodesmata induced by developmental, biotic, and abiotic signals. *Protoplasma* **225,** 67–76.

McDaniel CN. 1996. Developmental physiology of floral initiation in *Nicotiana tabacum* L. *Journal of Experimental Botany* **47,** 465–475.

Moran R. 1982. Formulae for determination of chlorophyllous pigments extracted with *N,N*-dimethylformamide. *Plant Physiology* **69,** 1376–1381.

Olesinski AA, Almon E, Navot N, Perl A, Galun E, Lucas WJ, Wolf S. 1996. Tissue specific expression of the *Tobacco mosaic virus* movement protein in transgenic potato plants alters plasmodesmal function and carbohydrate partitioning. *Plant Physiology* **111,** 541–550.

Rinne PL, van den Boogaard R, Mensink MG, Kopperud C, Kormelink R, Goldbach R, van der Schoot C. 2005. Tobacco plants respond to the constitutive expression of the tospovirus movement protein NS(M) with a heat-reversible sealing of plasmodesmata that impairs development. *The Plant Journal* **43,** 688–707.

Sagi G, Katz A, Guenoune-Gelbart D, Epel BL. 2005. Class 1 reversibly glycosylated polypeptides are plasmodesmal-associated proteins delivered to plasmodesmata via the Golgi apparatus. *The Plant Cell* **17,** 1788–1800.

Selth LA, Dogra SC, Rasheed MS, Randles JW, Rezaian MA. 2006. Identification and characterization of a host reversibly glycosylated peptide that interacts with the *Tomato leaf curl virus* V1 protein. *Plant Molecular Biology* **61,** 297–310.

Testasecca P, Wald FA, Cozzarin ME, Moreno S. 2004. Regulation of self-glycosylation of reversibly glycosylated polypeptides from *Solanum tuberosum*. *Physiologia Plantarum* **121,** 27–34.

Thomas CL, Bayer EM, Ritzenthaler C, Fernandez-Calvino L, Maule AJ. 2008. Specific targeting of a plasmodesmal protein affecting cell-to-cell communication. *PLoS Biology* **6,** e7.

Turgeon R, Webb JA. 1973. Leaf development and phloem transport in *Cucurbita pepo*: maturation of the minor veins. *Planta* **113,** 179–191.